Biosensors and Bioelectronics 25 (2010) 1989–1993

Contents lists available at ScienceDirect

Biosensors and Bioelectronics

journal homepage: www.elsevier.com/locate/bios

Short communication

Aligned carbon nanotubes on quartz substrate for liquid gated biosensing

Al. Palaniappan[a,*], W.H. Goh[a], J.N. Tey[a], I.P.M. Wijaya[a], S.M. Moochhala[a,b,c], B. Liedberg[a,c], S.G. Mhaisalkar[a,c,**]

[a] School of Materials Science and Engineering, Nanyang Technological University, Singapore 639798, Singapore
[b] DSO National Laboratories, 27 Medical Drive, Singapore 117510, Singapore
[c] Centre for Biomimetic Sensor Science, 50 Nanyang Drive, Singapore 637553, Singapore

ARTICLE INFO

Article history:
Received 18 September 2009
Received in revised form
26 November 2009
Accepted 12 January 2010
Available online 18 January 2010

Keywords:
Biosensor
Single walled carbon nanotube
Field effect transistor
Liquid gating

ABSTRACT

A facile and high performance biosensing platform using aligned carbon nanotubes on quartz substrate is reported in this communication. Single walled carbon nanotubes are grown on quartz substrates by a chemical vapor deposition process and are characterized with field emission scanning electron microscopy and atomic force microscopy in order to verify the quality of the material. The quartz substrate is then directly used as a biosensor in a field effect transistor configuration. In order to demonstrate the sensing capabilities of the fabricated sensor devices, electronic detection of prostate specific antigen, a potential cancer biomarker, is carried out by adopting liquid gated configuration. A conductivity change due to the specific binding of target antigen with the immobilized receptor antibody demonstrates the sensing capabilities of the fabricated device. Sub-nM detection sensitivities have been obtained using the adopted direct immunoassay approach, which shows that the device responds to clinically relevant concentration regimes.

1. Introduction

Carbon nanotubes (CNTs) have emerged to be an exciting class of materials for biosensing applications owing to their unique electrical and physical properties (Saito et al., 1998). Over the recent years, real time electronic detection of biomolecules, chemical species and gas molecules has been reported using functionalized CNT-based transistors (Kong et al., 2000). In most of these cases, random network of single walled carbon nanotubes (SWCNTs) are grown on Si/SiO_2 substrates using chemical vapor deposition (CVD) process. The material is subsequently modified with receptor molecules for detection of the analyte of interest (Villamizar et al., 2008; Pandana et al., 2008; Li et al., 2005; Tey et al., 2009; Sánchez-Acevedo et al., 2009; Gruner, 2006; Heller et al., 2008). SWCNT liquid gated field effect transistor (LGFET) sensing mechanism involves interaction between adsorbed analytes and SWCNT thereby altering the current flow through the SWCNT (drain current, I_d) depending on the charges associated with the adsorbed analyte via electrostatic gating, Schottky barrier, capacitance, and mobility modulation effects, which are characterized by a threshold voltage shift, I_d variations at zero gate voltage, transfer characteristic gradient variation and I_d reduction at positive and negative gate voltages, respectively (Gruner, 2006; Heller et al., 2008). It has previously been reported that in liquid gated CNT devices, the dominant mechanism is related to electrostatic gating which results in the reduction of the I_d upon adsorption of the biomolecules on the CNTs (Heller et al., 2008). Owing to the superior electrical properties, aligned SWCNT are usually preferred over random networks of SWCNT for enhanced device performance (Kocabas et al., 2005). However, growing high density of aligned tubes on Si/SiO_2 substrates still poses a significant challenge. Several attempts have been made to generate high density of aligned tubes on Si/SiO_2 substrates including flow assisted growth (Huang et al., 2007), solution deposition process (Meitl et al., 2004), transferring of aligned CNT to Si/SiO_2 substrate (Li et al., 2007), etc. For instance, considerable efforts have been devoted to the development of techniques capable of transferring tubes grown on quartz substrate to Si/SiO_2 substrates in order to fabricate high performance transistor devices using conventional back/top gated configuration (Kang et al., 2007a). However, most of these methodologies are cumbersome and result in poor transfer efficiency and thereby poor device performances. In this communication, we report a simple and a high performance biosensing platform using SWCNT grown on quartz substrates. The proposed sensing platform uses quartz directly as the supporting substrate for biosensing thereby eliminating the need for transferring SWCNT to Si/SiO_2 substrates. Successful electronic detection of prostate specific antigen (PSA), a potential cancer biomarker demonstrates the sensing capabilities of the fabricated devices.

* Corresponding author. Tel.: +65 67906748; fax: +65 67909081.
** Corresponding author at: School of Materials Science and Engineering, Nanyang Technological University, Singapore 639798, Singapore.
E-mail addresses: alps@ntu.edu.sg (Al. Palaniappan), subodh@ntu.edu.sg (S.G. Mhaisalkar).

0956-5663/$ – see front matter © 2010 Elsevier B.V. All rights reserved.
doi:10.1016/j.bios.2010.01.009

2. Experimental

All the reagents used for CNT growth, including the catalyst, $Co(C_2H_3O_2)_2{\cdot}4H_2O$ (cobalt(II) acetate tetrahydrate, ACS reagent, ≥98%) were purchased from Sigma–Aldrich and used without further purification. Prostate specific antigen (PSA), anti-PSA (a-PSA) and bovine serum albumin (BSA) were purchased from U.S. biological. ST-cut quartz substrates were obtained from Hoffman Materials Inc. and are subsequently annealed for 8 h at 900 °C. After ultrasonication in acetone and isopropyl alcohol for 10 min and in deionized water for 5 min, the wafers were blown dry with high-purity nitrogen. Cobalt acetate catalyst was either spin coated or drop coated on quartz substrates. SWCNTs are then grown on quartz substrates using ethanol CVD process as reported previously (Huang et al., 2004). In brief, after 10 min oxidation at 850 °C in a quartz tube furnace, the catalyst was reduced to pure Co metal at 925 °C under the flow of H_2 (200 sccm) for 10 min. SWCNTs were synthesized by bubbling Ar/H_2 (flow rate of 100 sccm/50 sccm) through a ethanol (carbon source) bottle. CVD for 30 min resulted in aligned SWCNTs along quartz surface as illustrated in Fig. 1a (Kocabas et al., 2007).

3. Results and discussion

Fig. 1a and b shows the field emission scanning electron microscope (FESEM, JSM-6340F, operated at 1 kV) image of SWCNT grown on quartz and Si/SiO_2 substrates, respectively. It can be observed from Fig. 1a that aligned tubes are generated on quartz surface compared to the random network of tubes on Si/SiO_2 surface (Fig. 1b) under similar growth conditions. This alignment minimizes the tube to tube contact resistance associated with network devices, thereby improving the transconductance and sensitivity and ultimately the overall performance of the device (Roberts et al., 2009; Reid, 2007). Fig. 1c and d shows the higher magnification AFM image (Scanning Probe Microscopy System, Dimension 3100) of the generated aligned tubes and its corresponding section analysis. Fig. 1c illustrates the alignment degree and the tube density of the SWCNT on quartz substrates. Approximately 4 tubes/μm are obtained using the adopted protocol, which is comparable to the previous reports (Kocabas et al., 2007). The section analysis (Fig. 1d) reveals that tubes of diameter ~1.5–2 nm are obtained under the adopted growth conditions.

Fig. 2 shows schematically, the proposed quartz field effect transistor (FET) device using partially aligned SWCNT as the conducting channel. About 4 mm wide, 100 nm thick Au source and drain electrodes are fabricated on the quartz substrates, perpendicular to the direction of nanotube alignment. The spacing between the electrodes is 175 μm. Random network and quartz transistor devices, corresponding to SWCNT morphology shown in Fig. 1a and b, respectively, are then obtained upon manual removal of tubes surrounding the electrodes region using solvents such as acetone. Liquid gating configuration is adopted for real time electronic detection of biomolecules (Kruger et al., 2001). Gate potential is applied via a reference electrode (3 M KCl) (FLEXREF from World Precision Instruments) and a voltage bias of 10 mV is applied between source and drain electrodes. As illustrated in Fig. 2, a PDMS reservoir confines the liquid in between source and drain electrodes for gating the transistor.

After sufficient characterization of SWCNT growth, electrical measurements for detection of PSA were conducted in order to validate the sensing capabilities of the fabricated device. The a-

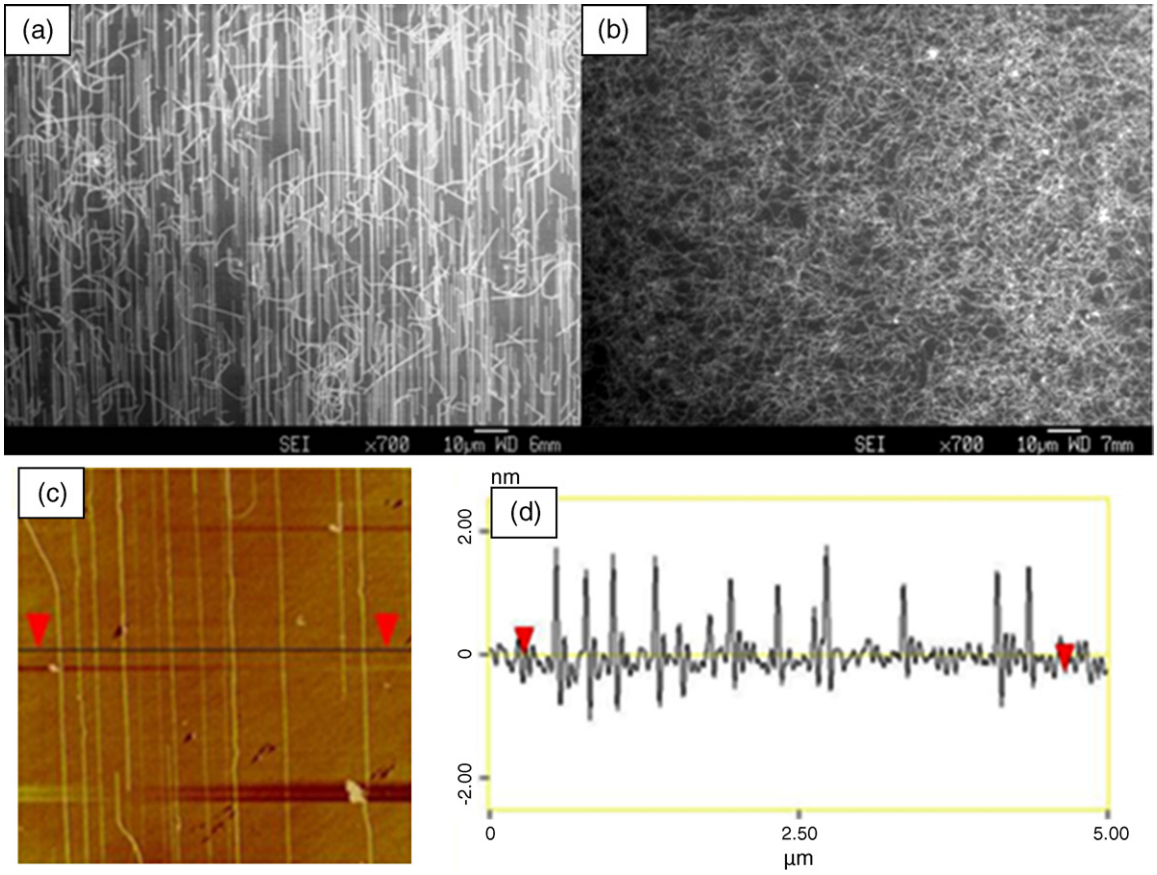

Fig. 1. FESEM images illustrating generated SWCNT alignment on quartz substrate (a) in comparison to Si/SiO_2 substrate (b). (c) AFM image shows that approximately 4 tubes/μm are obtained under the adopted growth conditions and the corresponding section analysis (d) further confirms aligned tube growth with diameters in the range of 1.5–2 nm.

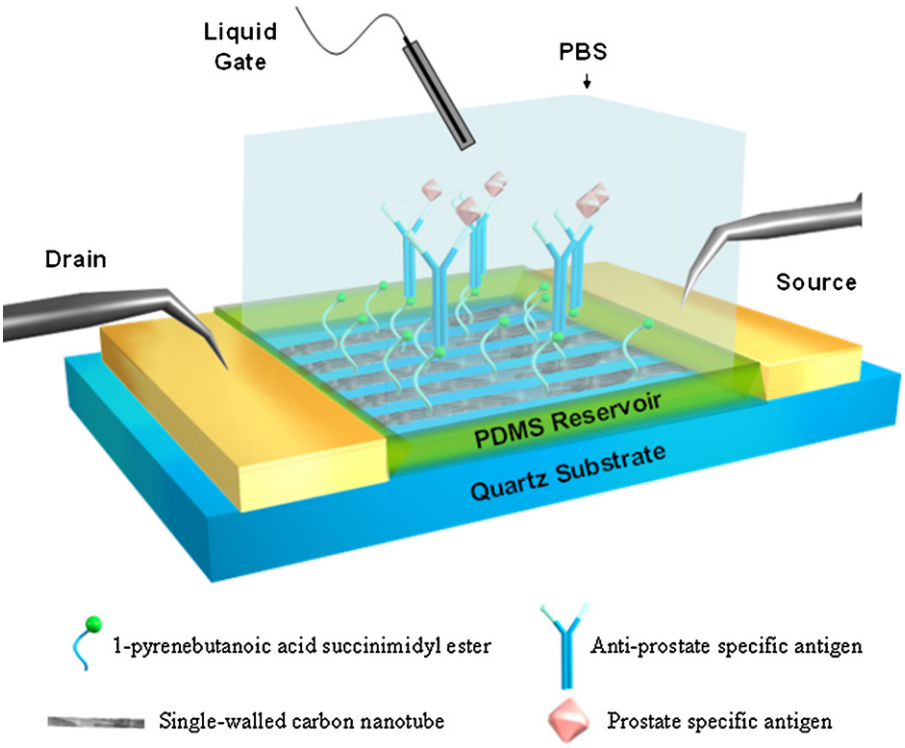

Fig. 2. Schematic of SWCNT sensor on quartz substrate for real time electronic detection of biomolecules; transistor electrodes are fabricated perpendicular to the growth direction and the quartz substrate is directly used as biosensors by adopting liquid gating configuration.

PSA is immobilized on the SWCNT using 1-pyrenebutanoic acid succinimidyl ester (PBSE) as linkers (Chan et al., 2001). In brief, the quartz device is incubated with 1% polyethylene glycol (PEG) in phosphate buffer solution (PBS) for 30 min in order to block the quartz substrate area not covered by SWCNT and thereby to achieve substrate passivation and to eliminate non-specific binding (NSB). The device is then incubated with 5 mM PBSE (in phosphate buffer, pH ~7.4) for 1 h followed by incubation for 90 min with a mixture of 10 μM a-PSA and 0.1% Tween in order to tether the a-PSA on SWCNT. Finally, the device is thoroughly rinsed several times with the PBS to remove loosely bound a-PSA.

The transfer characteristics measurements (drain current, I_d *vs* gate voltage, V_g) of the aligned and random network SWCNT on quartz and Si/SiO_2 substrates, respectively, are obtained using a methodology similar to a previous report (Kruger et al., 2001). A small voltage bias of 10 mV is applied between the source and drain electrodes and the current flowing through the SWCNT (I_d) is continuously monitored while sweeping the gate voltage (V_g). It could be observed from Fig. 3a that both random network and aligned devices show normal transistor behavior. However, mobility (μ) of the quartz device, estimated using a methodology reported earlier (Ozel et al., 2005; Tey et al., 2009), is significantly higher than the Si/SiO_2 device. The higher mobility of the quartz device ($\mu \sim 80\,cm^2/Vs$; assuming 4 tubes/μm from AFM image) in comparison with the conventional Si/SiO_2 device ($\mu \sim 30\,cm^2/Vs$) is indicative of its superior device performance as mobility is directly proportional to the device transconductance that leads to a larger change in I_d (dI_d) upon binding of the analyte. Fig. 3b shows the kinetic measurements recorded by tracking I_d at a fixed V_g (I_d *vs* time, at V_g of −0.3 V). The device was rinsed several times with the buffer solution (PBS + 0.1% Tween). The drain current upon attaining stable current response after a-PSA immobilization is taken as the reference for sensing measurements. The device was incubated with 100 nM BSA in order to evaluate the selectivity of the fabricated device. Anti-PSA is specific to PSA and therefore BSA would not adhere to immobilized anti-PSA. Hence, influence of physisorption of BSA or other biomolecules on quartz substrate or on SWCNT that would influence the sensor response, could be evaluated. The device was then rinsed with buffer solution and exposed to different concentrations of PSA, simultaneously recording the sensor response. Fig. 3b illustrates that I_d of the quartz device remains unaffected upon injection of 100 nM BSA (BSA in PBS with 0.1% Tween) and also upon several rinses with the buffer solution, confirming successful substrate passivation, but drops significantly upon injection of different concentrations of PSA (PSA in PBS with 0.1% Tween). This suggests that PSA selectively binds to immobilized a-PSA and subsequently modulates the conductance of SWCNT and thereby demonstrating the sensing capabilities of the device. Since PSA has positive surface charge potential (Villoutreix et al., 1994) it would shift the conductance curve to more negative gate voltages upon specific binding to a-PSA. This is in agreement with previous report regarding adsorption of positively charged species leading to a reduction in the drain current (I_d) due to electrostatic interaction between the adsorbed species and the SWCNT (Heller et al., 2008).

Fig. 3c shows the PSA sensor response of the conventional Si/SiO_2 device deposited with random networks of SWCNT functionalized with a-PSA. The drain current shifts upon injection of PSA (Fig. 3d) demonstrates that the quartz device exhibits better sensor response, at least by a factor of 3, when compared with a conventional Si/SiO_2 device prepared using the same growth conditions as that of the quartz device. The enhancement in the quartz device response could be attributed to the SWCNT alignment that minimizes the tube to tube contact resistance and to its high device mobility. As shown in Fig. 3d, the fabricated device exhibits reasonable reproducibility mainly influenced by the uniformity in SWCNT synthesis, which is the one of the concerns of current CNT research. However, reproducibility could further be improved upon sensor response normalization (Tey et al., 2009; Wijaya et al., 2010). Further screening for cancer may be required for elevated PSA levels in serum in the order of >~4 ng/ml (>~150 pM). A limit of detection (LOD), of ~30 pM and ~200 pM, for quartz and Si/SiO_2, respectively,

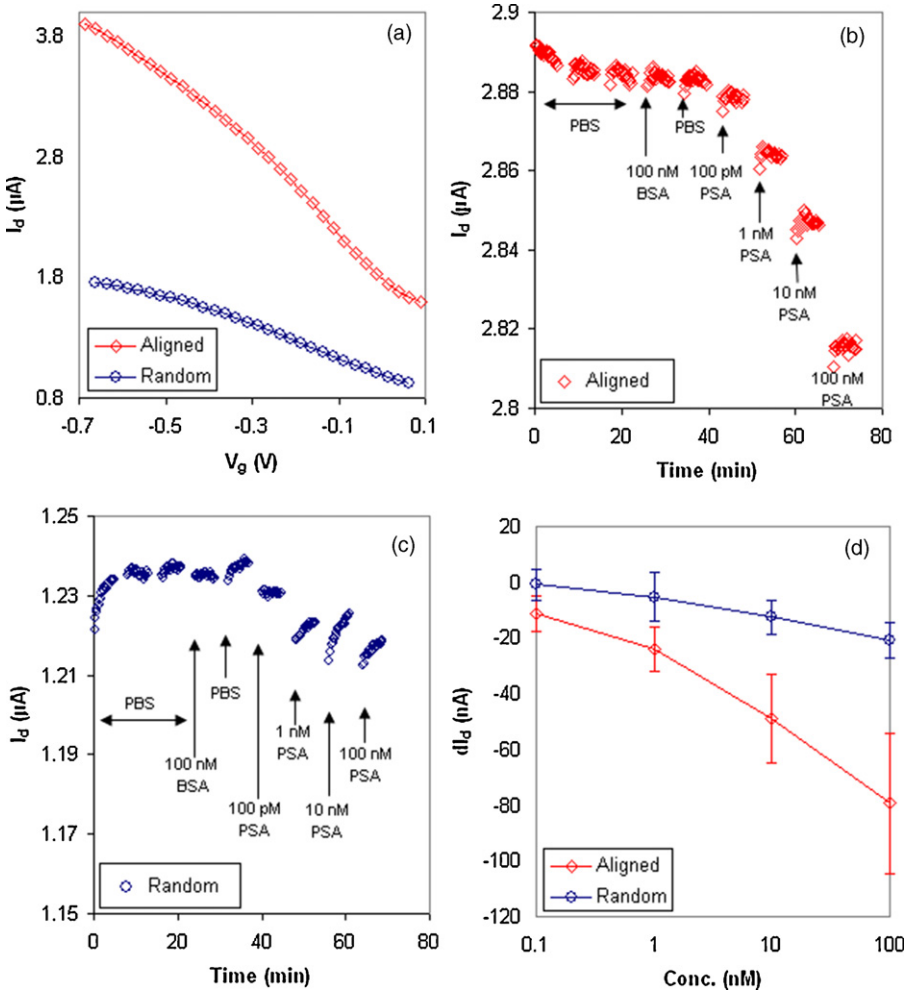

Fig. 3. Transfer characteristics measurement of quartz and Si/SiO_2 device (a)–(c), the corresponding kinetic measurements for different concentrations of PSA at fixed gate voltage of −300 mV. The average values of drain current shifts ($n = 5$) upon PSA introduction, illustrating that the sensor response of the fabricated quartz device is significantly higher than the conventional Si/SiO_2 devices. I_d shift of ~12 nA is observed for 100 pM PSA injection for the quartz device (d), ~3 times the LOD, further confirms that the quartz device responds to clinically relevant concentration regimes when compared to conventional Si/SiO_2 devices.

has been calculated using $3\sigma/S$ approach (Torsi et al., 2008), where σ is the standard deviation of device response in buffer solution without analytes (1.192 nA and 2.825 nA for quartz and Si/SiO_2 device, respectively) and S is the sensitivity, the slope of the sensor response (Fig. 3d) in the linear low concentration range. The obtained LOD and drain current shifts upon PSA injection are better than previous reports using conventional Si/SiO_2 devices (Li et al., 2005; Heller et al., 2008). The sensing and characterization results demonstrate the direct use of quartz as a supporting substrate in CNT-based biosensors. Since sub-nM detection sensitivities have been obtained using the adopted direct immunoassay approach, it could be concluded that the fabricated quartz device responds to clinically relevant concentration regimes (Kelloff et al., 2004). Further enhancement in the sensitivity would be possible by pursuing approaches that include enrichment of the semiconducting tubes in the FETs by electrical burn-off or chemical treatment means (Kang et al., 2007b), competitive assays (Wijaya et al., 2010) and nanoparticles based approaches (Dong et al., 2008). Some of these methodologies form future ongoing work and will be communicated.

4. Conclusions

In summary, the proposed methodology would be an ideal platform to fabricate biosensors with superior sensing performances, especially considering the recent advances in generating high density of perfectly aligned SWCNT on quartz substrates. Furthermore, since liquid gating configuration is adopted, the proposed device could be used for real time electronic detection of biomolecules. Detection of nM quantities of PSA was accomplished using the developed platform, which is comparable to the sensitivities of benchmark protein detection systems as ELISA. Besides being highly sensitive, the developed device eliminates the need for expensive equipment, high operational cost, long and tedious experimental procedures associated with the current benchmark protein detection systems. Various ultra-sensitive biosensors also could be fabricated using the proposed quartz FET by appropriately functionalizing the SWCNT.

References

Chan, R.J., Zhang, Y., Wang, D., Dai, H., 2001. J. Am. Chem. Soc. 123, 3838–3839.
Dong, X., Lau, C.M., Lohani, A., Mhaisalkar, S.G., Kasim, J., Shen, Z., Ho, X., Rogers, R.A., Li, L.J., 2008. Adv. Mater. 20, 2389–2393.
Gruner, G., 2006. Anal. Bioanal. Chem. 384, 322–335.
Heller, I., Janssens, A.M., Mannik, J., Minot, E.D., Lemay, S.G., Dekker, C., 2008. Nano Lett. 8, 591–595.
Huang, L., Cui, X., White, B., O'Brien, S.P., 2004. J. Phys. Chem. B 108, 16451–16456.
Huang, L., Jia, Z., O'Brien, S., 2007. J. Mater. Chem. 17, 3863–3874.
Kang, S.J., Kocabas, C., Kim, H.S., Cao, Q., Meitl, M.A., Khang, D.Y., Rogers, R.A., 2007a. Nano Lett. 7, 3343–3348.
Kang, S.J., Kocabas, C., Ozel, T., Shim, M., Pimparkar, N., Alam, M.A., Rotkin, S.V., Rogers, R.A., 2007b. Nat. Nanotechnol. 2, 230–236.

Kelloff, G.J., Coffey, D.S., Chabner, B.A., Dicker, A.P., Guyton, K.Z., Nisen, P.D., Soule, H.R., D'Amico, A.V., 2004. Clin. Can. Res. 10, 3927–3933.
Kocabas, C., Hur, S.H., Gaur, A., Meitl, M.A., Shim, M., Rogers, R.A., 2005. Small 1, 1110–1116.
Kocabas, C., Kang, S.J., Ozel, T., Shim, M., Rogers, R.A., 2007. J. Phys. Chem. C 111, 17879–17886.
Kong, J., Franklin, N.R., Zhou, C., Chapline, M.G., Peng, S., Cho, K., Dai, H., 2000. Science 287, 622–625.
Kruger, M., Buitelaar, M.R., Nussbaumer, T., Schonenberger, C., Forro, L., 2001. Appl. Phys. Lett. 78, 1291–1293.
Li, C., Curreli, M., Lin, H., Lei, B., Ishikawa, F.N., Datar, R., Cote, R.J., Thompson, M.E., Zhou, C., 2005. J. Am. Chem. Soc. 127, 12484–12485.
Li, S., Yan, Y., Liu, N., Chan-Park, M.B., Zhang, Q., 2007. Small 3, 616–621.
Meitl, M.A., Zhou, Y., Gaur, A., Jeon, S., Usrey, M.L., Strano, M.S., Rogers, R.A., 2004. Nano Lett. 4, 1643–1647.
Ozel, T., Gaur, A., Rogers, R.A., Shim, M., 2005. Nano Lett. 5, 905–911.
Pandana, H., Aschenbach, K.H., Lenski, D.R., Fuhrer, M.S., Khan, J., Gomez, R.D., 2008. IEEE Sens. J. 8, 655–660.
Reid, T., 2007. Nat. Nanotechnol. doi:10.1038/nnano.2007.272.
Roberts, M.E., LeMieux, M.C., Bao, Z., 2009. ACS Nano 3, 3287–3293.
Saito, R., Dresselhaus, G., Dresselhaus, M.S., 1998. Physical Properties of Carbon Nanotubes. Imperial College Press, London.
Sánchez-Acevedo, Z.C., Riu, J., Rius, F.X., 2009. Biosens. Bioelectron. 24, 2842–2846.
Tey, J.N., Wijaya, I.P.M., Wang, Z., Goh, W.H., Palaniappan, Al., Mhaisalkar, S.G., Rodriguez, I., Dunham, S., Rogers, R.A., 2009. Appl. Phys. Lett. 94, 013107–013113.
Torsi, L., Farinola, G.M., Marinelli, F., Tanese, M.S., Omar, O.H., Valli, L., Babudri, F., Palmisano, F., Zambonin, P.G., Naso, F., 2008. Nat. Mater. 7, 412–417.
Villamizar, R.A., Maroto, A., Rius, F.X., Inza, I., Figueras, M.J., 2008. Biosens. Bioelectron. 24, 279–283.
Villoutreix, B.O., Getzoff, E.D., Griffin, J.H., 1994. Protein Sci. 3, 2033–2044.
Wijaya, I.P.M., Tey, J.N., Gandhi, S., Boro, R., Palaniappan, Al., Goh, W.H., Rodriguez, I., Suri, C.R., Mhaisalkar, S.G., 2010. Lab Chip. doi:10.1039/b918566f.